JOC The Journal of Organic Chemistry

Article

pubs.acs.org/joc

# Minimalist Synthetic Host with Stacked Guanidinium Ions Mimics the Weakened Hydration Shells of Protein−protein Interaction Interfaces

Xing Wang, Joshua Post, Dennis K. Hore,* and Fraser Hof*

Department of Chemistry, University of Victoria, P.O. Box 3600, Victoria V8W 3V6, Canada

Supporting Information

**ABSTRACT:** Protein surfaces are complex solutes, and protein−protein interactions are specifically mediated by surface motifs that modulate solvation shells in poorly understood ways. We report herein a supramolecular host that is designed to mimic one of the most important recognition motifs that drives protein−protein interactions, the stacked arginine side chain. We show that it binds its guests and displays good selectivity in the highly competitive medium of pure, buffered water. We use a combination of experimental studies of binding and molecular dynamics simulations to build a cohesive picture of how this biomimetic host achieves the feat. The presence of the stacking element next to the guanidinium groups causes a decrease in the number of host−water hydrogen bonds, a decrease in the density of water around the host, and a decrease in water−water hydrogen bonds near the host. Experimental data using mixed organic/aqueous solvent systems confirm that this host relies on the hydrophobic effect in a way that the two control hosts do not. Our simulations and analysis provide detailed information on the linkage between (de)hydration and binding events in water in a way that could be applied to many aqueous supramolecular systems.

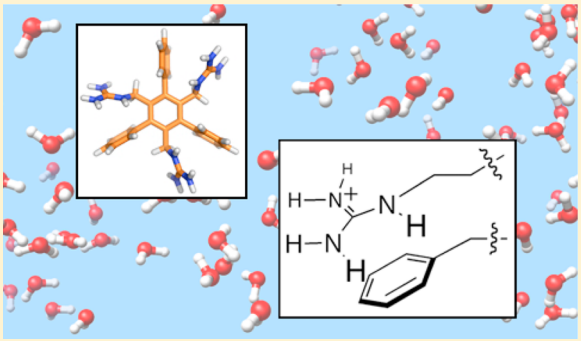

## INTRODUCTION

Protein−protein interactions (PPIs) rely on the exclusion of water from interacting residues.[1−3] It has been shown that despite the large size of PPI interfaces it is small, modular clusters of residues that weaken the hydration shells around key polar contacts to drive binding.[3−5] Arginine residues are frequently found at the cores of protein-interaction interfaces,[6−13] where they are far more common than, for example, lysine residues,[14] and where they contribute a disproportionately large amount of binding energy to PPIs.[12] Protein structural surveys and functional studies show that the hydrophilic side chains of arginine residues are often found next to hydrophobic aromatic side chains and that these cation−$\pi$ interactions are energetically favorable (Figure 1a).[15−20]

Synthetic guanidinium-containing hosts are widely used in anion recognition.[21,22] The idea that guanidinium ions in proteins (and at protein-interaction interfaces) often exist in environments that are sheltered from water by neighboring residues is well understood,[22,23] but synthetic scaffolds that specifically probe the effect of placing the guanidinium ions in proximity to aromatic or hydrophobic elements are relatively rare and typically have not operated in pure water.[24−28] We report herein a biomimetic synthetic host, **1**, that presents three such pairs of guanidinium-aryl binding elements about a central 1,3,5-triphenylbenzene core, a new variation on the well-known trisubstituted benzene scaffolds[29,30] that have been used for the creation of diverse supramolecular hosts (Figure 1b). We find that it can bind a complementary guest in pure water and at high buffer concentrations and that the presence of aromatic elements directly adjacent to the guanidinium binding elements imparts both guest selectivity and solvation effects that are not observed for control hosts (**2** and **3**) that contain the exact same guanidinium ion binding elements but are lacking the phenyl rings. We use molecular dynamics simulations to gain detailed information on the solvating water structure around each host, and we show that the simple array of functional groups in **1** is sufficient to encode some of the hydration effects that are characteristic of protein−protein interfaces.

## RESULTS

The synthesis for **1** (Scheme 1) starts with the bromination of known 2,4,6-trimethyl-1,3,5-triphenylbenzene **4**[31] with *N*-bromosuccinimide, giving tris(bromomethyl) product **5** in 86% yield. Heating compound **5** with $NaN_3$ in acetone/water gave the corresponding triazide (not shown) in 80% yield, but reductions attempted with $NaBH_4$, $LiAlH_4$, $PPh_3$, $H_2$, and Pd/C under various temperatures and presures all failed to give complete (or any) reaction to the desired triamine, presumably because of the steric hindrance of the triphenylbenzene scaffold. Instead, compound **5** was converted directly into tris(aminomethyl)benzene **6** by treatment with aqueous $NH_3$ followed by concentration to dryness. Unpurified **6** was used

**Received:** September 4, 2013
**Published:** December 12, 2013

   dx.doi.org/10.1021/jo401949s | J. Org. Chem. 2014, 79, 34−40

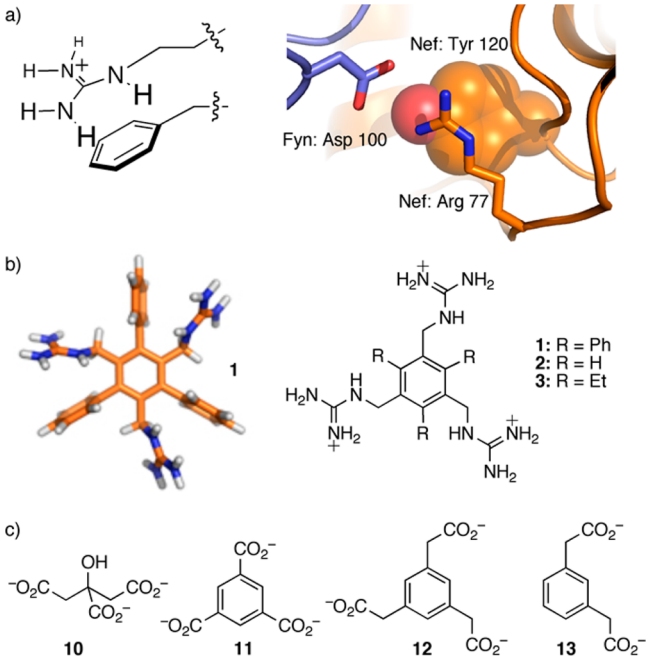


**Figure 1.** (a) $\pi$-stacked arginine motifs (left) are commonly found as key recognition elements at protein-interaction interfaces (right; exemplary structural data taken from PDB entry 1AVZ). (b) Host **1** was designed to display three stacked guanidinium ions (PM3-minimized structure), whereas hosts **2** and **3** serve as controls. All hosts were studied as their tri(hydrochloride) salts. (c) Guests used in this study; all guests were used as their $Bu_4N^+$ salts and prepared as previously reported.[25,33]

**Scheme 1. Synthesis of Hosts 1–3**[a]

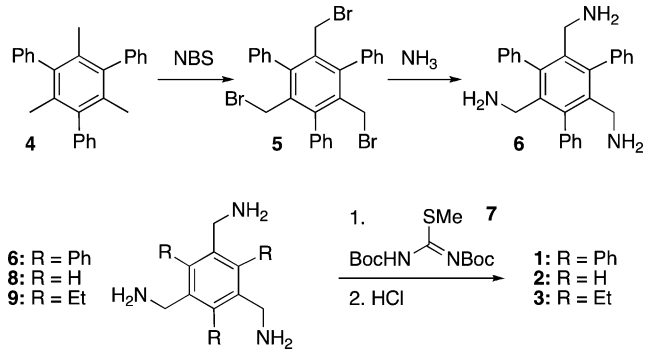


[a]See the Experimental Section for details.

directly in a reaction with *N,N′*-bis(*tert*-butoxycarbonyl)-2-methyl-2-thiopseudourea (**7**) to give the Boc-protected host, which could be purified by chromatography and then treated with HCl to provide desired host compound **1** cleanly as the HCl salt. Two control hosts bearing the same array of three guanidinium groups upon an unsubstituted benzene (**2**) and the classical 1,3,5-triethylbenzene scaffold (**3**) were prepared from corresponding triamines **8**[32] and **9**[30] in a similar manner (see the Supporting Information).

Tricarboxylates **10**–**12** (Figure 1c) were chosen as binding partners that complement the 3-fold presentation of guanidinium binding elements by receptors **1**–**3**. $^1$H NMR titrations were used to obtain the binding constants in $D_2O$ buffered at pD 7.8 with 100 mM Tris (Figure 2). The $K_{assoc}$ values, determined by fitting chemical-shift data to a 1:1 binding isotherm, are generally in the low $10^2$ $M^{-1}$ range (Table 1), as expected for hosts of this type operating under highly competitive buffer concentrations.[34] Receptor **1**, bearing stacked guanidinium elements, binds guest **12** ($K_{assoc}$ = 320 $M^{-1}$) but shows no detectable binding ($K_{assoc}$ < 10 $M^{-1}$) of closely related tricarboxylates **10** and **11**. Receptors **2** and **3** are more promiscuous, binding all three tricarboxylates with similar $K_{assoc}$ values, with guest **12** slightly disfavored relative to the two other guests for host **3**. Hosts **1**–**3** do not measurably bind the common dicarboxylates glutarate, Cbz-glutamate, and glutamate under these conditions, nor do they bind guest **13**, the dicarboxylate analogue of the strongest guest, **12**. This suggests strongly that all three carboxylates are required to drive complex formation.

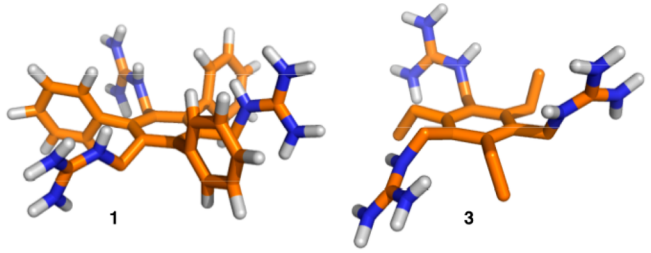


**Figure 2.** Snapshots of hosts **1** (pictured in a syn conformation) and **3** (in an anti conformation) from MD simulations.

**Table 1. Association Constants ($M^{-1}$) in 100 mM Tris-Buffered $D_2O$**[a]

| | citrate (**10**) | benzene-1,3,5-tricarboxylate (**11**) | benzene-1,3,5-triacetate (**12**) |
|---|---|---|---|
| **1** | <10 | <10 | 320 ± 130 |
| **2** | 190 ± 60 | 340 ± 130 | 240 ± 130 |
| **3** | 220 ± 45 | 325 ± 20 | 145 ± 25 |

[a]Values reported are averages determined by 2–4 replicate $^1$H NMR titrations. Uncertainties reported are standard deviations. Hosts were used as their $Cl^-$ salts, and guests were used as their $Bu_4N^+$ salts. See the Supporting Information for details.

To obtain a direct view of solvation effects, $^1$H NMR titrations were carried out in a 50:50 (v/v) mixture of the same Tris-buffered $D_2O$ and $CD_3OD$. The decreased polarity of this medium allows us to examine directly the relative contributions of electrostatic effects (which become stronger in a less polar medium) and the hydrophobic effect (which becomes weaker upon addition of an organic cosolvent). Surprisingly, the three triguanidinium hosts respond to the intrusion of methanol in markedly different ways: stacking host **1** shows weakened binding with some loss of selectivity, unsubstituted host **2** shows similar affinities as in pure buffered $D_2O$, and triethyl-substituted host **3** experiences a significant increase in association constant for all three guests (Table 2). We conclude that the triethyl host relies heavily upon electrostatic forces for binding (also supported by prior data on the effect of added salts for a related triethylbenzene-derived host),[34,35] whereas the binding of guests by the new triphenyl host is driven primarily by the hydrophobic effect, which is attenuated upon addition of MeOH.

Molecular dynamic simulations of hosts **1**–**3** in explicit water (see the Supporting Information for details) were used to give us a deeper understanding of the conformations and hydration shells of these hosts. The simulation data were first analyzed to


dx.doi.org/10.1021/jo401949s | J. Org. Chem. 2014, 79, 34–40

**Table 2. Association Constants ($M^{-1}$) in 50:50 (v/v) MeOD/100 mM Tris-Buffered $D_2O$[a]**

| | citrate (**10**) | benzene-1,3,5-tricarboxylate (**11**) | benzene-1,3,5-triacetate (**12**) |
|---|---|---|---|
| **1** | 20 ± 10 | <10 | 70 ± 10 |
| **2** | 220 ± 140 | 520 ± 250 | 440 ± 50 |
| **3** | 4360 ± 320 | 540 ± 5 | 770 ± 160 |

[a]Values reported are averages determined by 2−4 replicate $^1$H NMR titrations. Uncertainties reported are standard deviations. Hosts were used as their $Cl^-$ salts, and guests were used as their $Bu_4N^+$ salts. See the Supporting Information for details.

understand the conformations of all three $C_3$-symmetric hosts to check for changes in geometry that might affect guest binding. Conformations can be broadly grouped into those with three guanidiniums on the same face of the central ring (syn) that are preorganized for engaging a guest and those with one guanidinium directed to the opposite face of the ring (anti). The rate of dynamic exchange between conformations (flip rate) slows as the size of the groups neighboring the recognition arms increases (Table 3), but the parameter that

**Table 3. Conformational Parameters for Hosts 1−3 Derived from Molecular Dynamics Simulations in Explicit Water[a]**

| | flip rate at 300 K (flips/ns) | flip rate at 400 K (flips/ns) | percent of time in syn conformation at 300 K | percent of time in syn conformation at 400 K |
|---|---|---|---|---|
| **1** | <0.005[b] | 0.2 | n.a.[b] | 25 |
| **2** | 170 | 290 | 24 | 27 |
| **3** | 2.3 | 11.3 | 11 | 20 |

[a]The syn conformation is defined as any conformation in which all three guanidinium binding elements are on the same face of the central benzene ring (all three $CH_2$−N bond vectors >10° from the plane defined by the central ring), and the anti conformation is any conformation in which one of the three guanidiniums is on the opposite face of the central benzene ring (two $CH_2$−N bond vectors >10° above and one $CH_2$−N bond vector >10° below the plane defined by the central ring). The flip rate arises from counting exchange events between syn and anti conformations during simulations lasting 200 ns. [b]No conformational flips were observed even during a 200 ns simulation of **1** at 300 K, setting an upper limit for the flip rate and precluding the determination of the preferences for the percent of time in the syn conformation by this method.

can influence binding thermodynamics, the time-averaged degree of preorganization, is similar for all three hosts. Hosts **1** and **2** spend approximately the statistically predicted 25% of the time in the syn conformation. Triethyl host **3**, which is, in principle, sterically programmed to occupy a syn conformation,[29,36,37] in fact spends slightly less than the predicted amount of time in that conformation (11% at 300 K and 20% at 400 K). We have recently reported that, in general, sterically geared ethyl-substituted tripodal hosts of this type often do not display the strong preorganization that is expected of them.[38] In any case, the differences in preorganization between **1**, **2**, and **3** are so small that they would not be expected to affect binding energies based on the entropic costs of preorganization. This conclusion is supported by the fact that when complexes form the binding affinities displayed by all three hosts in pure buffered water are of a similar order of magnitude.

The simulation data for hosts **1**−**3** were further analyzed to gain insight into how these hosts interact with the water in their own hydration shells. An identical simulation on the small hydrophobic solute benzene was also performed to allow comparisons. The number of host−water hydrogen bonds was tested by checking all 200 000 frames from the 200 ns simulations at 300 K using standard distance and angle criteria (donor−acceptor distance <3.5 Å and donor hydrogen-acceptor angle 180° ± 30°). On average, host **1** participates in fewer H-bonds to water (3.30) than do host **3** (3.58) and host **2** (3.92). The density of water molecules as a function of distance from each host and from benzene was also examined and found to be markedly different from one solute to another (Figure 3). In spite of their abilities to hydrogen bond to water

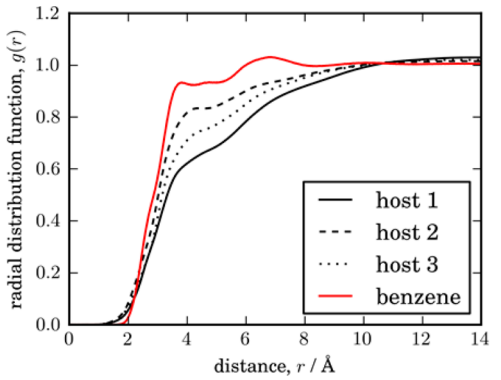


**Figure 3.** Density of water molecules as a function of distance (measured from heavy atoms) from hosts **1**−**3** and from benzene, as determined by molecular dynamics simulations in explicit water at 300 K.

molecules, all of the guanidinium-containing hosts experienced an overall lower density of solvating water than did the simple hydrophobic solute benzene. Host **1** is surrounded by a lower density of water molecules than either of the other two hosts, and significant differences in density persist out to a distance of 10 Å where all four water density profiles arrive at the density of bulk water (1.0 g/mL).

We sought to understand this result by examining the shape of water-density profiles in three dimensions. Figure 4 provides maps of the water density centered about the core benzene ring of each host and of benzene. The right column is a cut in the plane of the central benzene ring; the left column is cut perpendicular to this plane. In the case of the benzene molecule, the in-plane (IP) slice shows a roughly symmetrical density of water in a single solvation shell, whereas the out-of-plane (OP) region shows a very high density of water situated in a small region directly above and below the ring (which corresponds to the putative binding site for a guest making multiple salt bridges to any of these hosts). This is in agreement with what has been observed in previous experiments[39] and simulations.[40] The three hosts investigated in this study show essentially the same behavior as benzene for the out-of-plane water density except that they have a greatly diminished first hydration shell with more than 2.5 times lower water density. The out-of-plane hydration profile of host **1** contains the smallest region of high density, a result that goes some way toward understanding the fact that it has the lowest density of solvating waters, as shown by the bulk density−distance profiles in Figure 3. Also noteworthy is that the regions of maximum density above and below the plane in unsubstituted host **2** have a significantly greater spatial extent than for the other two hosts. The in-plane water density (right column of Figure 4) is more complicated, with three hydration shells clearly evident


dx.doi.org/10.1021/jo401949s | J. Org. Chem. 2014, 79, 34−40

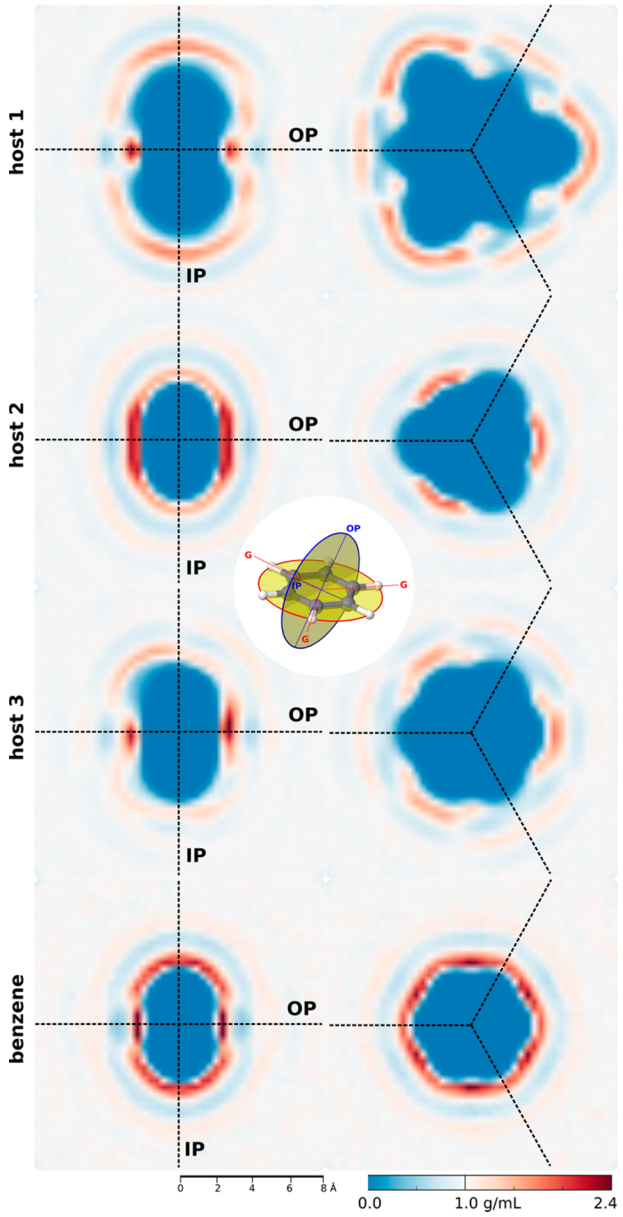


**Figure 4.** Water density surrounding hosts in the plane of the central benzene ring (right column) and a perpendicular plane (left column). The inset illustrates the location of the three guanidinium groups (G) and the axes both in the plane (IP) of the central benzene ring and out-of-the plane (OP). In each case, the water density has been displayed out to a radius of 8 Å from the central phenyl ring. No color (white) indicates a density of 1 g/mL, higher than bulk water density is indicated in red, and lower density, in blue.

for all hosts. The first partial hydration shell appears surrounding the R groups; the second partial shell occurs in the vicinity of the guanidinium groups (marked G in Figure 4). The final hydration shell, as expected, is relatively symmetrically distributed in the plane of the central benzene ring.

Finally, in an effort to determine the internal cohesion of solvating water shells, we determined the number of water–water hydrogen bonds within the pool of water molecules located ≤10 Å from each host and normalized the count to the total number of waters present in each host's solvation shell volume under examination. We determined the average number of water–water H-bonds in bulk water using our counting method to be 3.67 (in good agreement with reported values).[41,42] The waters around host **1** participated in only 2.67 water–water H-bonds per water molecule, whereas the values for **2** and **3** were 2.75 and 2.71, respectively. These values differ much less among the hosts than the host–water hydrogen bond counts. However, it is reassuring that the rank ordering of all three measures of water cohesion (water density profiles, water–host H-bond counts, and water–water H-bond counts) agree with each other. This gives a consistent picture of the differences between the dynamic shells of water around each host observed during the course of the simulations.

## DISCUSSION

Hosts **1**, **2**, and **3** show affinities for tricarboxylate guest **12** in pure buffered water that are generally similar (within 2–3-fold of each other), but host **1** shows a greater degree of guest selectivity than is seen in **2** or **3** in that it binds guests **10** and **11** much less strongly than it does guests **12**. Given the identical connectivity of guanidinium ions around the central core in each host and their similar conformational preferences revealed by MD simulations, it seems that the best explanation for these differences is in a change in the balance between contributions from weak interactions and the hydrophobic effect in the different host–guest complexes.

Among the weak interactions between hosts and guests, the most prominent to consider are aromatic–aromatic interactions and the combined electrostatic and hydrogen-bonding contact encoded by each carboxylate-guandinium salt bridge. The pendant aryl rings of **1** have some exposed edges that might enable edge–face interactions with aromatic guests **11** and **12**. However, triaryl host **1** forms complexes with **13** of similar strength to those formed by nonaryl-substituted **2** and **3**, offering evidence that the aryl rings of **1** are not making host–guest contacts that are directly responsible for the observed guest selectivities in water or for the changes in guest binding in methanol/water. All three hosts have identical guanidinium ion arrays for salt-bridge-mediated guest binding, but we think these are more likely to contribute to the observed changes in host–guest discrimination in different solvents (the shielding of charged groups from solvating water molecules by neighboring bulky groups is known to drive stronger interactions in pure water).

The solvation effects we observed are unusual and beg questions about the solvation of both the free and bound states. Simulations of the hosts alone provided us with useful insight into their structures and solvation shells in water. However, simulations of the intact complexes are not as informative; as expected, the complexes adopt a multitude of different structures over the course of hundreds of nanoseconds, and the roles of weak interactions and the stuctures of solvent shells in these very dynamic structures are much harder to break down in an informative way than are the simulations of the hosts alone. The experimental binding constants (combined with the observed solvent effects) lead us to speculate that the increased hydrophobic surface area of guest **12** relative to **10** and **11** might be the factor that drives it to form a tight complex with host **1** (the most hydrophobic of the hosts).

It is clear from these data that host **1** responds to the addition of organic solvent in a way that is dramatically different from the other two control hosts. The addition of an organic cosolvent is a more reliable and direct way to study solvation effects than the more traditional determinations of entropic/enthalpic contributions, which in fact cannot easily


dx.doi.org/10.1021/jo401949s | J. Org. Chem. 2014, 79, 34–40

separate out entropic/enthalpic contributions from solvent from those of binding interactions.[33] When an organic cosolvent is added, the dielectric constant of the medium is lowered (providing decreased screening and increased strength of electrostatic interactions), and the strength of hydrophobic effect is diminished. In the present case, the strongly increased potency of host **3** in MeOD/$D_2O$ indicates that its binding of guests is more dependent on electrostatic interactions. We can only speculate as to why this host should have such a strong dependence on electrostatic interactions. We can rule out explanations based on differences in preorganization, but it is possible that this host allows closer (and more electrostatically driven) carboxylate−guanidinium contacts than do the others. The proof of such an interpretation would require X-ray structures for multiple complexes that we have been unable to obtain. In contrast, the decreased potency of host **1** demonstrates a much smaller role for electrostatic attraction and suggests a prominent role for the hydrophobic effect in the binding of guest **12** by **1** in pure buffered $D_2O$. This is also consistent with the fact that **12** is the most hydrophobic of the guests and **1** is the most hydrophobic of the hosts.

The roles of the $Bu_4N^+$ guest counterions (which were chosen to confer solubility in both aqueous and mixed organic/aqueous systems) are also worth discussion. These hydrophobic counterions have been seen to form strong complexes with neutral or anionic aromatic hosts in pure water,[43] but we have no evidence that such complexation exists between these tricationic hosts and the similarly charged $Bu_4N^+$. The solvation energies of the $Bu_4N^+$ ions and therefore their tendencies to aggregate are certainly different in each of these two solvent systems. We do not rule out the involvement of $Bu_4N^+$ as a peripheral participant in different host−guest complexes (especially in water). However, the large excess of $Na^+$ present in all binding buffers and the consistent use of the same $Bu_4N^+$ cations (and $Na^+$ buffers) for all guests would seem to rule out a role for the counterions in determining either (a) the guest selectivities exhibited by **1** in pure water or (b) the different responses of hosts **1** and **3** to the move from water into mixed organic/aqueous solvent.

The MD simulations provide a deeper insight into how the stacking elements in host **1** influence the hydration of its guanidinium-binding elements. Host **1** participates in the fewest host−water H-bonds of all three hosts even though each presents identical arrays of guanidinium ions to the solvent. The radial distribution functions in Figure 3 show that the decreased density of water caused by the stacking elements of host **1** extends far beyond the first hydrogen-bonded shell of hydrating waters and persists out to 10 Å from the host, which is well into its third sphere of hydration. There is also evidence in the simulations that there is only a very small number of waters occupying the binding surface of host **1** compared to the equivalent surfaces of hosts **2** and **3** or of benzene. Furthermore, the accounting of water−water interactions within the entire 10 Å radius sphere around each host shows that water−water hydrogen bonding is decreased significantly from bulk values in the vicinity of each guanidinium-containing host and that the effect is the strongest for host **1**. In contrast, the density of water around benzene is very near 1 g/mL (±10%) in its entire solvation sphere. These experimental and MD data all paint a consistent picture of host **1** as a species that weakens the hydration of its highly hydrophilic guanidinium ions in a way that closely related hosts **2** and **3** do not.

Triethyl-substituted hosts, such as **2**, are common in the literature.[29,30,38] A guanidinium-functionalized relative of host **2** also binds to citrate, and an exhaustive study of the enthalpies and entropies of binding has been carried out.[34] The binding of citrate by the host and also a subsequent formation of a 2:1 host−guest complex in small amounts were shown to be driven by electrostatic interactions involving the guanidinium ions. In a high-concetration buffer, the binding affinity decreased, as expected (and as observed for many electrostatically driven complexes). In numerous other studies involving charged binding partners, the addition of organic solvent to water (decreasing polarity) has generally caused an increase in binding affinities.[33] Here, our system shows an unexpected trait in which the response of the $K_{assoc}$ value to the introduction of an organic cosolvent depends strongly on the nature of the groups that neighbor the key binding elements.

## CONCLUSIONS

We have attempted here to provide a basic understanding of (a) how water is structured around complex solutes that are mixtures of hydrophilic guanidinium ions and with different neighboring groups and (b) how these differences in water structure produce functional differences in binding behavior. Arginines recognize partners through both cation−$\pi$ interactions[15,20] and hydrogen bonding.[44] In proteins, they frequently experience both types of interaction simultaneously (and this is especially true at protein-interaction interfaces[13]), essentially becoming a complex solute whose interactions with water must depend strongly on their hybrid charged and hydrophobic nature. However, only a handful of model studies have examined the interplay of both stacking and hydrogen bonding acting simultaneously around a single guanidinium ion.[25,45−49] Our results here point to a distinct role for hydration in differentiating the behavior of a stacked from a nonstacked guanidinium ion. It is not clear from these data if the aromaticity of the stacking elements in **1** is responsible for its behavior or if the facial juxtaposition of other kinds of hydrophobic elements (such as a large aliphatic amino acid side chain) with a guanidinium ion would be sufficient for these complex solvation effects to emerge, but it is clear that the simple arrangement of alternating hydrophobic and hydrophilic functional groups around the core of **1** creates a surface that is more weakly hydrated (in terms of surrounding water density and surrounding water structure) than either the completely hydrophobic benzene or more hydrophilic analogues **2** and **3**. In this way, this minimalist model mimics the interplay between hydration effects and arginine recognition that is proposed to operate at PPI interfaces, which are known to include small modular structures that help to shed hydrating waters from key polar residues.[1−5] It is intriguing to consider how other compact, stacked amphiphilic model systems like compound **1** might perform at the difficult task of achieving selective molecular recognition in water.

## EXPERIMENTAL SECTION

**Tris(bromomethyl) Precursor 5.** A mixture of compound **4**[31] (309 mg, 0.88 mmol) and *N*-bromosuccinimide (917 mg, 5.15 mmol) in $CH_2Cl_2$ (50 mL) was irradiated with a sunlamp under $N_2$ for 24 h and then concentrated to dryness on a rotary evaporator. The resulting yellow solid was triturated with methanol to give the product as a pale-brown solid (439 mg, 85%). mp 214 °C. $^1$H NMR ($CDCl_3$, 300 MHz): 3.92 (s, 6H), 7.46 (s, 15H). $^{13}$C NMR ($CDCl_3$, 75 MHz): 30.4,


dx.doi.org/10.1021/jo401949s | J. Org. Chem. 2014, 79, 34−40

128.2, 129.6, 135.1, 136.8, 144.0. IR (thin film): 776m, 700m. EI-MS ($M^+$, $m/z$): found for $C_{27}H_{21}Br_3$, 582/584/586/588.

**Boc-Protected Precursor to Triphenyl-Substituted Host 1.** Tribromide **5** (600 mg, 1.0 mmol) was dissolved in a mixture of dioxane (40 mL) and concentrated aqueous ammonia (8 mL) and stirred at room temperature under $N_2$ for 24 h. The reaction was concentrated to dryness using a rotary evaporator to give the crude product as a pale-yellow powder that was used without further purification. $^1$H NMR (DMSO-$d_6$, 300 MHz): 3.39 (s, 4H), 7.34−7.59 (15H). A portion of crude triphenyl-substituted triamine **6** (295 mg, 0.75 mmol) was then dissolved in MeOH (30 mL). The solution was treated first with $Et_3N$ (0.8 mL, 5.7 mmol) and then with *N*,*N*′-Bis(*tert*-butoxycarbonyl)-*S*-methylisothiourea (1.00 g, 3.4 mmol). The mixture was stirred at room temperature under $N_2$ overnight and then concentrated to dryness on a rotary evaporator (**Caution:** *stench*!). The resulting solid was purified by column chromatography ($SiO_2$, 7:3 hexanes/EtOAc) to yield the product as a white solid (265 mg, 31%). mp 98−100 °C. $^1$H NMR ($CDCl_3$, 300 MHz): 1.38 (s, 27H, Boc), 1.49 (s, 27H, Boc), 4.05 (d, $J$ = 6.0 Hz, 6H, $CH_2$), 7.22−7.27 (m, 15H, phenyl), 7.94 (s, 3H, NH), 11.11 (s, 3H, NH). $^{13}$C NMR ($CDCl_3$, 300 MHz): 29.9, 30.1, 43.0, 80.5, 84.5, 129.2, 130.1, 130.9, 135.7, 139.8, 146.3, 154.8, 156.4, 164.9. IR (thin film): 3408m, 3335m, 2978m, 1719 s, 1637s, 1615s(sh), 1155s, 1129, 809s, 776s, 742s, 703s. HR-ESI-TOF-MS ($MNa^+$, $m/z$): calcd for $C_{60}H_{81}N_9O_{12}Na$, 1142.5902; found, 1142.5911.

**Triphenyl-Substituted Host 1.** The Boc-protected host (above) (168 mg, 0.15 mmol) was dissolved in a mixture of glacial AcOH (9 mL) and concentrated aqueous HCl (0.4 mL), and the mixture was stirred at room temperature under $N_2$ overnight. Concentration to dryness on a rotary evaporator followed by repeated treatments wth HCl and concentration to dryness gave the product as its hydrochloride salt as a white powder (94 mg, 100%). mp 284 °C dec. $^1$H NMR ($CD_3OD$, 300 MHz): 3.75 (s, 6H), 7.44−7.51 (m, 15H). $^{13}$C NMR ($CD_3OD$, 75 MHz): 43.0, 129.3, 129.7, 130.4, 133.7, 138.8, 146.3, 157.4. IR (thin film) 3335m, 3408s(sh), 1719m, 1637s, 704m. HR-ESI-TOF-MS ($MH^+$, $m/z$): calcd for $C_{30}H_{34}N_9$, 520.2932; found, 520.2928.

**Boc-Protected Precursor to Unsubstituted Host 2.** 1,3,5-Tris(aminomethyl)benzene **8** (228 mg, 0.83 mmol) was dissolved in MeOH (40 mL). $Et_3N$ (0.5 mL, 3.5 mmol) was added prior to addition of *N*,*N*′-bis(*tert*-butoxycarbonyl)-*S*-methylisothiourea (1.08 g, 3.74 mmol) as a solid. The reaction was stirred under $N_2$ at room temperature for 24 h and then concentrated to dryness on a rotary evaporator (**Caution:** *stench*!). Purification of the residue by column chromatography (7:3 hexanes/EtOAc) yielded the product as a white solid (369 mg, 50%). mp 116−118 °C. $^1$H NMR ($CDCl_3$, 300 MHz): 1.38 (s, 27H), 1.49 (s, 27H), 4.61 (d, $J$ = 6.0 Hz, 6H), 7.16 (s, 3H), 8.58 (s, 3H), 11.54 (s, 3H). $^{13}$C NMR ($CDCl_3$, 75 MHz): 28.0, 28.3, 44.7, 79.4, 83,2, 126.6, 138.4, 153.1, 156.2, 163.6. IR (thin film): 3425s(sh), 3333s, 2978m, 1721m, 1640s, 1620s(sh), 1411m, 1327m, 1157s, 1132s, 809w, 773w, 736w. HR-ESI-TOF-MS ($MH^+$, $m/z$): calcd for $C_{42}H_{70}N_9O_{12}$, 892.5144; found, 892.5135.

**Unsubstituted Host 2.** A mixture of Boc-protected precursor (above) (159 mg, 0.18 mmol), AcOH (9 mL), and concentrated aqueous HCl (0.4 mL) was stirred at room temperature under $N_2$ overnight and then concentrated to dryness on a rotary evaporator. Repeated treatments with HCl followed by concentration to dryness gave the product as its hydrochloride salt as a pale-yellow solid (71 mg, 100%). mp 280 °C dec. $^1$H NMR ($CD_3OD$, 300 MHz): 4.48 (s, 6H), 7.32 (s, 3H). $^{13}$C NMR ($CD_3OD$, 75 MHz): 45.7, 126.9, 139.2, 174.3. IR (thin film) 3346m, 3166s(sh), 1651s. HR-ESI-TOF-MS ($MH^+$, $m/z$): calcd for $C_{12}H_{22}N_9$, 292.1998; found, 292.2003.

**Boc-Protected Precursor to Triethyl-Substituted Host 3.** Triamine **9** (220 mg, 0.62 mmol) was dissolved in MeOH (10 mL). $Et_3N$ (0.7 mL, 4.96 mmol) was added prior to addition of *N*,*N*′-bis(*tert*-butoxycarbonyl)-*S*-methylisothiourea (1.08 g, 3.72 mmol) as a solid. The reaction was stirred under $N_2$ at room temperature for 24 h and then concentrated to dryness on a rotary evaporator (**Caution:** *stench*!). Purification of the residue by column chromatography (9:1 to 7:3 hexanes/EtOAc) yielded the product as a white solid (190 mg, 32%). mp 138−140 °C. $^1$H NMR ($CDCl_3$, 300 MHz): 1.11 (t, $J$ = 7.4 Hz, 9H), 1.37 (s, 27H), 1.47 (s, 27H), 2.63 (q, $J$ = 7.4 Hz, 6H), 4.52 (d, $J$ = 3.9 Hz, 6H), 8.04 (s, 3H), 11.44 (s, 3H). $^{13}$C NMR ($CDCl_3$, 75 MHz): 16.3, 23.2, 28.0, 28.3, 39.9, 79.4, 83.0, 131.4, 145.0, 152.9, 155.5, 163.6. HR-ESI-TOF-MS ($MH^+$, $m/z$): calcd for $C_{48}H_{82}N_9O_{12}$, 976.6083; found, 976.6057.

**Triethyl-Substituted Host 3.** The Boc-protected precursor (above) (40 mg, 0.04 mmol) was dissolved in a mixture of glacial AcOH (2 mL) and concentrated aqueous HCl (0.1 mL). After stirring at room temperature overnight, the reaction was concentrated to dryness. Repeated treatments wth HCl followed by concentration to dryness gave the product as its hydrochloride salt as a white powder (20 mg, 100%). mp > 300 °C. $^1$H NMR (DMSO-$d_6$, 300 MHz): 1.07 (t, $J$ = 7.3 Hz, 9H), 2.60 (q, $J$ = 7.3 Hz, 6H), 4.28 (d, $J$ = 3.2 Hz, 6H), 6.5−8.0 (br, 10H). $^{13}$C NMR ($CD_3OD$, 75 MHz): 16.5, 24.2, 41.2, 131.6, 146.3, 158.5. HR-ESI-TOF-MS ($MH^+$, $m/z$): calcd for $C_{18}H_{34}N_9$, 376.2937; found, 376.2934.

**Binding Studies.** NMR solvents and reagents were used as obtained from Cambridge Isotope Laboratories. NMR titrations were carried out at 298 K on a Brüker Avance AV500 spectrometer. All solutions were prepared using $D_2O$ containing 100 mM Tris buffer, adjusted to a reading on the pH meter of 7.8 by addition of NaOD or DCl solutions in $D_2O$. The 50:50 (v/v) buffer/$CD_3OD$ solvent system was premixed to ensure that host and guest solutions contained precisely matched solvent compositions. Guests were prepared as their $Bu_4N^+$ salts as previously reported.[2S,33] Solutions of the host (0.5−2 mM) were titrated by solutions containing a higher concentration of the guest (5−50 mM) and a matched concentration of host. To obtain the best possible accuracy, titrations were carried out at the maximum concentrations allowable by the solubility of the individual components. Inverse titrations of host into guest were also carried out in a similar manner as permitted by the solubility of the host. Chemical-shift data were fit to a 1:1 binding isotherm (Figure S1) using an Excel spreadsheet made available by Sanderson,[50] and the $K_{assoc}$ values from the movement of multiple protons and from replicate titrations (both normal and inverse) were averaged and reported with their standard deviations.

**Molecular Dynamics Simulations.** Isothermal−isobaric molecular dynamics simulations were performed with the GROMACS package.[51] Systems consisted of a separate single molecule of each host in a cubic cell filled with SPC/E water.[52] The cell for host **1** had a length of 30.0 Å with 881 water molecules (reproducing a bulk water density of 1 g/mL), host **2** was in a 29.8 Å length cell with 872 waters, and host **3** was in a 30.1 Å cell with 877 waters. Each system was simulated with periodic boundary conditions. van der Waals and Coulombic forces were cutoff at a radius of 9.9 Å. Host intramolecular interactions and host−water interactions were handled using the OPLS-AA/L force field.[53] The energy of each system was minimized using the steepest-descent method implemented in GROMACS with a step size of 0.1 Å. Each simulation was equilibrated for 200 ps with different random velocities assigned to each of its atoms at start up to achieve overall temperatures of 300 or 400 K, which were maintained by coupling to a Berendsen thermostat;[54] pressure was maintained at 1.01325 bar with a Berendsen barostat.[54] Following equilibration, runs were performed for 200 ns at each temperature, collecting data every 0.1 ps. The integrator step size during equilibrations and runs was 1 fs. Analysis of host−water hydrogen bonds, water−water hydrogen bonds, and radial density functions of water for each host were carried out by examination of each of 200 000 frames of the 200 ns simulations at 300 K using standard tools available in GROMACS and home-written scripts. Distance/angle criteria are as discussed in the article.

Two-dimensional water-density maps were created by first locating the atoms of the central benzene ring in each frame of the simulation, taking periodic boundary conditions into consideration. The Cartesian coordinates of all water molecules in the frame were then rotated into the frame of this benzene ring. Waters were binned in three dimensions according to the location of their (rotated) oxygen atoms, with a bin resolution of 0.05 Å. Slices were cut across two


dx.doi.org/10.1021/jo401949s | J. Org. Chem. 2014, 79, 34−40

planes of the histogram, parallel and perpendicular to the central ring, as indicated in the inset of Figure 4.

## ■ ASSOCIATED CONTENT

### Supporting Information

$^{1}$H and $^{13}$C NMR for all new compounds and exemplary data for NMR titrations. This material is available free of charge via the Internet at http://pubs.acs.org.

## ■ AUTHOR INFORMATION


### Corresponding Authors

*E-mail: dkhore@uvic.ca (D.K.H.).
*E-mail: fhof@uvic.ca (F.H.).


### Notes

The authors declare no competing financial interest.

## ■ ACKNOWLEDGMENTS

This work was supported by NSERC Discovery Grants to D.K.H. and F.H. We thank Christine Greenwood for expert NMR assistance and Travis Trudeau and Sandra Roy for their help in setting up the molecular simulations. F.H. is a Canada Research Chair.

## ■ REFERENCES


(1) Li, Y. L.; Huang, Y. P.; Swaminathan, C. P.; Smith-Gill, S. J.; Mariuzza, R. A. *Structure* **2005**, *13*, 297.
(2) Sundberg, E. J.; Urrutia, M.; Braden, B. C.; Isern, J.; Tsuchiya, D.; Fields, B. A.; Malchiodi, E. L.; Tormo, J.; Schwarz, F. P.; Mariuzza, R. A. *Biochemistry* **2000**, *39*, 15375.
(3) Keskin, O.; Ma, B. Y.; Nussinov, R. *J. Mol. Biol.* **2005**, *345*, 1281.
(4) Reichmann, D.; Rahat, O.; Albeck, S.; Meged, R.; Dym, O.; Schreiber, G. *Proc. Natl. Acad. Sci. U.S.A.* **2005**, *102*, 57.
(5) Reichmann, D.; Rahat, O.; Cohen, M.; Neuvirth, H.; Schreiber, G. *Curr. Opin. Struct. Biol.* **2007**, *17*, 67.
(6) Crowley, P. B.; Golovin, A. *Proteins: Struct., Funct., Bioinf.* **2005**, *59*, 231.
(7) Inglis, S. R.; Stojkoski, C.; Branson, K. M.; Cawthray, J. F.; Fritz, D.; Wiadrowski, E.; Pyke, S. M.; Booker, G. W. *J. Med. Chem.* **2004**, *47*, 5405.
(8) Vetter, I. R.; Arndt, A.; Kutay, U.; Gorlich, D.; Wittinghofer, A. *Cell* **1999**, *97*, 635.
(9) Arold, S.; Franken, P.; Strub, M. P.; Hoh, F.; Benichou, S.; Benarous, R.; Dumas, C. *Structure* **1997**, *5*, 1361.
(10) Conte, L. L.; Chothia, C.; Janin, J. *J. Mol. Biol.* **1999**, *285*, 2177.
(11) Zhou, H. X.; Shan, Y. *Proteins: Struct., Funct., Bioinf.* **2001**, *44*, 336.
(12) Bogan, A. A.; Thorn, K. S. *J. Mol. Biol.* **1998**, *280*, 1.
(13) Crowley, P. B.; Golovin, A. *Proteins: Struct., Funct., Bioinf.* **2005**, *59*, 231.
(14) Chakrabarti, P.; Janin, J. *Proteins: Struct. Funct. Genet.* **2002**, *47*, 334.
(15) Gallivan, J. P.; Dougherty, D. A. *Proc. Natl. Acad. Sci. U.S.A.* **1999**, *96*, 9459.
(16) Flocco, M. M.; Mowbray, S. L. *J. Mol. Biol.* **1994**, *235*, 709.
(17) Brocchieri, L.; Karlin, S. *Proc. Natl. Acad. Sci. U.S.A.* **1994**, *91*, 9297.
(18) Mitchell, J. B. O.; Nandi, C. L.; McDonald, I. K.; Thornton, J. M.; Price, S. L. *J. Mol. Biol.* **1994**, *239*, 315.
(19) Hughes, R. M.; Waters, M. L. *J. Am. Chem. Soc.* **2006**, *128*, 12735.
(20) Ma, J. C.; Dougherty, D. A. *Chem. Rev.* **1997**, *97*, 1303.
(21) Best, M. D.; Tobey, S. L.; Anslyn, E. V. *Coord. Chem. Rev.* **2003**, *240*, 3.
(22) Blondeau, P.; Segura, M.; Perez-Fernandez, R.; de Mendoza, J. *Chem. Soc. Rev.* **2007**, *36*, 198.
(23) Crowley, P. B.; Golovin, A. *Proteins* **2005**, *59*, 231.
(24) Haj-Zaroubi, M.; Mitzel, N. W.; Schmidtchen, F. P. *Angew. Chem., Int. Ed.* **2002**, *41*, 104.
(25) Wang, X.; Sarycheva, O. V.; Koivisto, B. D.; McKie, A. H.; Hof, F. *Org. Lett.* **2007**, *10*, 297.
(26) Echavarren, A.; Galan, A.; Lehn, J. M.; De Mendoza, J. *J. Am. Chem. Soc.* **1989**, *111*, 4994.
(27) Orner, B. P.; Salvatella, X.; Quesada, J. S.; de Mendoza, J.; Giralt, E.; Hamilton, A. D. *Angew. Chem., Int. Ed.* **2002**, *41*, 117.
(28) Haj-Zaroubi, M.; Schmidtchen, F. P. *ChemPhysChem* **2005**, *6*, 1181.
(29) Hennrich, G.; Anslyn, E. V. *Chem.—Eur. J.* **2002**, *8*, 2219.
(30) Kilway, K. V.; Siegel, J. S. *Tetrahedron* **2001**, *57*, 3615.
(31) Yang, J. S.; Huang, H. H.; Lin, S. H. *J. Org. Chem.* **2009**, *74*, 3974.
(32) Grawe, T.; Schrader, T.; Zadmard, R.; Kraft, A. *J. Org. Chem.* **2002**, *67*, 3755.
(33) Linton, B. R.; Goodman, M. S.; Fan, E.; van Arman, S. A.; Hamilton, A. D. *J. Org. Chem.* **2001**, *66*, 7313.
(34) Rekharsky, M.; Inoue, Y.; Tobey, S.; Metzger, A.; Anslyn, E. *J. Am. Chem. Soc.* **2002**, *124*, 14959.
(35) Metzger, A.; Lynch, V. M.; Anslyn, E. V. *Angew. Chem., Int. Ed. Engl.* **1997**, *36*, 862.
(36) Iverson, D. J.; Hunter, G.; Blount, J. F.; Damewood, J. R.; Mislow, K. *J. Am. Chem. Soc.* **1981**, *103*, 6073.
(37) Stack, T. D. P.; Hou, Z. G.; Raymond, K. N. *J. Am. Chem. Soc.* **1993**, *115*, 6466.
(38) Wang, X.; Hof, F. *Beilstein J. Org. Chem.* **2012**, *8*, 1.
(39) Suzuki, S.; Green, P. G.; Bumgarner, R. E.; Dasgupta, S.; Goddard, W. A.; Blake, G. A. *Science* **1992**, *257*, 942.
(40) Raschke, T. M.; Levitt, M. *J. Phys. Chem. B.* **2004**, *108*, 13492.
(41) Soper, A. K.; Bruni, F.; Ricci, M. A. *J. Chem. Phys.* **1997**, *106*, 247.
(42) Matsumoto, M. *J. Chem. Phys.* **2007**, *126*, 054503.
(43) Whiting, A. L.; Neufeld, N. M.; Hof, F. *Tetrahedron Lett.* **2009**, *50*, 7035.
(44) Baker, E. N.; Hubbard, R. E. *Prog. Biophys. Mol. Biol.* **1984**, *44*, 97.
(45) Dvornikovs, V.; Smithrud, D. B. *J. Org. Chem.* **2002**, *67*, 2160.
(46) Thompson, S. E.; Smithrud, D. B. *J. Am. Chem. Soc.* **2002**, *124*, 442.
(47) Rensing, S.; Arendt, M.; Springer, A.; Grawe, T.; Schrader, T. *J. Org. Chem.* **2001**, *66*, 5814.
(48) Takeuchi, T.; Kosuge, M.; Tadokoro, A.; Sugiura, Y.; Nishi, M.; Kawata, M.; Sakai, N.; Matile, S.; Futaki, S. *ACS Chem. Biol.* **2006**, *1*, 299.
(49) Orner, B. P.; Salvatella, X.; Quesada, J. S.; de Mendoza, J.; Giralt, E.; Hamilton, A. D. *Angew. Chem., Int. Ed.* **2002**, *41*, 117.
(50) Sanderson, J. M. The Sanderson Group Home Page. http://www.dur.ac.uk/j.m.sanderson/science/downloads.html.
(51) van der Spoel, D.; Lindahl, E.; Hess, B.; Groenhof, G.; Mark, A. E.; Berendsen, H. J. C. *J. Comput. Chem.* **2005**, *26*, 1701.
(52) Berendsen, H. J. C.; Grigera, J. R.; Straatsma, T. P. *J. Phys. Chem.* **1987**, *91*, 6269.
(53) Kaminski, G. A.; Friesner, R. A.; Tirado-Rives, J.; Jorgensen, W. L. *J. Phys. Chem. B.* **2001**, *105*, 6474.
(54) Berendsen, H. J. C.; Postma, J. P. M.; van Gunsteren, W. F.; DiNola, A.; Haak, J. R. *J. Chem. Phys.* **1984**, *81*, 3684.